Geometry and Intrinsic Tilt of a Tryptophan-Anchored Transmembrane α-Helix Determined by ^{2}H NMR

Patrick C. A. van der Wel,* Erik Strandberg,† J. Antoinette Killian,† and Roger E. Koeppe, II*

*Department of Chemistry and Biochemistry, University of Arkansas, Fayetteville, Arkansas 72701 USA; and †Department of Biochemistry of Membranes, Center for Biomembranes and Lipid Enzymology, Institute of Biomembranes, Utrecht University, 3584 CH Utrecht, The Netherlands

ABSTRACT We used solid-state deuterium NMR spectroscopy and an approach involving geometric analysis of labeled alanines (GALA method) to examine the structure and orientation of a designed synthetic hydrophobic, membrane-spanning α-helical peptide in phosphatidylcholine (PC) bilayers. The 19-amino-acid peptide consists of an alternating leucine and alanine core, flanked by tryptophans that serve as interfacial anchors: acetyl-GWW$(LA)_6$LWWA-ethanolamine (WALP19). A single deuterium-labeled alanine was introduced at different positions within the peptide. Peptides were incorporated in oriented bilayers of dilauroyl- (di-C12:0-), dimyristoyl- (di-C14:0-), or dioleoyl- (di-C18:1_c-) phosphatidylcholine. The NMR data fit well to a WALP19 orientation characterized by a distinctly nonzero tilt, $\sim$4° from the membrane normal, and rapid reorientation about the membrane normal in all three lipids. Although the orientation of WALP19 varies slightly in the different lipids, hydrophobic mismatch does not seem to be the dominant factor causing the tilt. We suggest rather that the peptide itself has an inherently preferred tilted orientation, possibly related to peptide surface characteristics or the disposition of tryptophan indole anchors relative to the lipids, the peptide backbone, and the membrane/water interface. Additionally, the data allow us to define more precisely the local alanine geometry in this membrane-spanning α-helix.

INTRODUCTION

Understanding the structures and lipid interactions of integral membrane proteins represents an important challenge. Genome analysis predicts that 20–30% of open reading frames in complex organisms encode membrane proteins (Wallin and Von Heijne, 1998). Although several dozen crystal structures of complex membrane proteins have been solved, the crystallization of membrane proteins remains a significant practical problem that limits the number of available structures. Furthermore, the crystallization conditions often involve membrane-mimetic conditions instead of actual membrane lipids. Even in successfully determined structures the lipid membrane itself may not be visible, and so the actual orientation of the protein components with respect to the lipids cannot be measured directly and is therefore usually deduced based on assumptions.

The interiors of membrane proteins are similar in hydrophobicity to those of soluble proteins and are packed just as tightly (White and Wimley, 1999). Their properties differ in that amino acids of outer surfaces of membrane proteins, facing the lipid acyl chains, are hydrophobic, whereas the outer surfaces of water-soluble proteins are hydrophilic. For proteins that have multiple membrane-spanning segments (α-helices or β-sheets), the relative orientations of those segments presumably can be determined largely by protein-protein interactions. For membrane-spanning α-helices in bundles, the helices typically tilt significantly with respect to the bilayer normal, averaging $\sim$22° $\pm$ 11° within several sets of bundle proteins that have been analyzed (Bowie, 1997; Ulmschneider and Sansom, 2001). For proteins in which lipid interactions dominate, such as those with a single membrane-spanning α-helix, the situation is less clear. Model lipid/protein systems that employ single membrane-spanning helices would be useful for investigating these lipid interactions and the resulting intrinsic tilt of the peptide helix.

Important differences between soluble proteins and membrane proteins arise because of the dielectric gradient across a membrane, the properties of the membrane/water interface, and the directional orientation of membrane-spanning proteins. The fluid-mosaic model (Singer and Nicolson, 1972) allows membrane proteins to diffuse within the bilayer, yet restricts them firmly to the bilayer plane and permits little motion in the perpendicular direction. An anchoring relative to the bilayer normal could be accomplished through specific interactions at the interface. To investigate a variety of lipid interactions, we have developed a useful model system of tryptophan-anchored, uncharged, membrane-spanning peptides, sometimes designated as WALP peptides, in which pairs of Trp residues near the N- and C-terminals flank a highly α-helical $(Leu-Ala)_n$ hydrophobic core (Killian et al., 1996). The WALP peptides orient strongly in a transmembrane direction (Killian et al., 1996), seem to experience little or no aggregation under typical experimental conditions (de Planque et al., 1998), and influence lipid phase behavior as a function of the relative hydrophobic matching of the lipid and peptide

Submitted October 5, 2001, and accepted for publication May 13, 2002.

Address reprint requests to Dr. Patrick C. A. van der Wel, Department of Chemistry and Biochemistry, Chemistry Bldg. 101, University of Arkansas, Fayetteville, AR 72701. Tel.: 479-575-3181; Fax: 479-575-4049; E-mail: pvander@uark.edu or rk2@uark.edu.

0006-3495/02/09/1479/10 $2.00

lengths (Killian et al., 1996; de Planque et al., 1999; van der Wel et al., 2000).

As in soluble proteins, internal hydrogen bonding of α-helices and β-sheets is important for membrane proteins and, in fact, even more important because of the energetic cost of burying a non-hydrogen-bonded peptide amide in a lipid bilayer (White and Wimley, 1999). The secondary structure elements of membrane proteins strongly resist denaturation and (to span the membrane) tend toward greater average lengths than in soluble proteins (Haltia and Freire, 1995). Members of the WALP peptide family were found to be highly α-helical based on circular dichroism (CD) and attenuated total reflection Fourier transform infrared spectroscopy (ATR-FTIR) measurements (de Planque et al., 2001). Furthermore, the backbone N-H bonds of the membrane-spanning α-helical $(Leu\text{-}Ala)_n$ core are very stable (for weeks) against solvent (^2H_2O) deuterium exchange (Demmers et al., 2000, 2001). CD spectra from oriented WALP peptide/lipid samples are consistent with peptides aligned in an orientation that is approximately parallel to the membrane normal (Killian et al., 1996). The polarized ATR-FTIR spectra additionally suggest that WALP peptides of a total length between 16 (WALP16) and 25 (WALP25) residues have tilt angles of less than 10° from the dimyristoylphosphatidylcholine (DMPC) bilayer normal (de Planque et al., 2001).

In this study, we use solid-state deuterium NMR spectroscopy to narrow the range and define more precisely the tilt of the 19-amino-acid (WALP19) member of the WALP peptide family, acetyl-GWWLALALALALALALWWA-ethanolamine, in three different bilayer-forming lipids, dilauroylphosphatidylcholine (DLPC), DMPC, and dioleoylphosphatidylcholine (DOPC). Single, specific alanines in WALP19 were labeled with deuterium, and the corresponding spectra were recorded using oriented, hydrated lipid/peptide samples. The results are consistent with a small but well defined helix tilt and spectral averaging about the bilayer normal but not about the helix axis. This ^2H NMR method for investigating the transmembrane helix orientation, based on the geometric analysis of labeled alanines (GALA) can complement other methods that include oriented ^{15}N NMR (Harzer and Bechinger, 2000), two-dimensional ^1H-^{15}N dipolar coupling/^{15}N chemical shift polarization inversion with spin exchange at the magic angle (Marassi and Opella, 2000; Wang et al., 2000), and site-specific infrared dichroism (Kukol and Arkin, 1999, 2000; Torres et al., 2000). A GALA-type approach was described before in the examination of the orientation and motion of the transmembrane domain of the epidermal growth factor (Jones et al., 1998). In addition to the peptide orientation, we also were able to refine the geometry of the alanine side chains with respect to the α-helical backbone.

MATERIALS AND METHODS

Materials

Fmoc-L-Ala Wang resin and Fmoc-protected amino acids were purchased from Advanced ChemTech (Louisville, KY) and NovaBiochem (San Diego, CA). Deuterated L-alanine-d_4 and deuterium-depleted water were obtained from Cambridge Isotope Laboratories (Andover, MA). DLPC (di-C12:0-PC), DMPC (di-C14:0-PC), and DOPC (di-C18:1_c-PC) were obtained from Avanti Polar Lipids (Alabaster, AL). 2,2,2-Trifluoroethanol was purchased from J.T. Baker (Phillipsburg, NJ), and methanol was from Burdick and Jackson (Muskogee, MI).

Peptide synthesis

The peptides were synthesized by solid-phase synthesis on an Applied Biosystems (Foster City, CA) 433A synthesizer using fastMoc chemistry (Greathouse et al., 1999, 2001). Beforehand, deuterated L-alanine-d_4 had to be coupled to an N-terminal Fmoc protecting group, as described in Greathouse et al. (1999). The peptide sequence was acetyl-$GWW(LA)_6LWWA$-ethanolamine, with ^2H-labeled alanines at position 5, 7, 9, 11, 13, or 15. Peptide identity and purity were confirmed by mass spectrometry and reversed-phase high-performance liquid chromatography.

Oriented NMR samples

The oriented NMR samples consist of macroscopically aligned lipid bilayers containing the peptides in a membrane-spanning orientation. These experiments were done at a 1:20 peptide/lipid ratio, but a test with a 1:40 peptide/lipid ratio yielded identical results. The procedure for aligning the samples was based on a number of previously published techniques (Cornell et al., 1988; Lee and Cross, 1994; Koeppe et al., 1996). A peptide-lipid mixture was prepared from 4 μmol of peptide and 80 μmol of lipid dissolved in trifluoroethanol and chloroform, respectively. The solvents were removed under nitrogen flow followed by drying under vacuum. After dissolution in 1 ml of either methanol or 95% methanol/5% water (v/v), the mixture was distributed over 40 glass plates ($4.8 \times 23 \times 0.07$ mm; Marienfeld Laboratory Glassware, Lauda-Königshofen, Germany). Solvents were removed by drying under vacuum ($\leq$0.010 torr) for 2 days. The sample plates were hydrated with an amount of deuterium-depleted water required for a 40% (w/w) hydration and immediately stacked together. Increased and faster alignment was obtained by applying some pressure to the stacked plates. The stack was inserted into a glass cuvette, empty glass slides were added if necessary to ensure a tight fit, and the cuvette was carefully sealed with quick-drying epoxy.

NMR measurements

All NMR measurements were performed at 40°C to ensure that the lipids are in the liquid crystalline phase. Lipid alignment within the samples was measured by oriented solid-state ^{31}P NMR with proton decoupling, using a custom-made ^{31}P NMR probe from Doty Scientific (Columbia, SC) and a Bruker AMX2 300 spectrometer, modified for wideline operation.

Oriented deuterium NMR experiments were performed using a quadrupolar echo pulse sequence with full phase cycling (Davis et al., 1976), with a 3-μs pulse time, 30–75-μs echo delay, and a 30-ms interpulse time. Experiments in which the interpulse time was varied from 30 to 900 ms showed no significant change in the spectra. The aligned samples were measured in two different orientations: with the normal to the lipid bilayers aligned either parallel to the applied magnetic field ($\beta = 0°$) or perpendicular to it ($\beta = 90°$). After application of a 100-Hz line-broadening to the spectra, the magnitude of the quadrupolar splitting ($|\Delta\nu_q|$) of each doublet was determined as the distance between the peak maxima.

TABLE 1 Definitions of structural parameters used in this manuscript

Parameter	Description
β	Angle between the membrane normal and the magnetic field
ε	Angle between the alanine side chain (C_α-C_β bond) and the helix axis
ρ	Rotational angle of the helix, defined relative to glycine 1
τ	Tilt angle of the helix, relative to the membrane normal
θ	Angle between labeled group (C_α-C_β bond) and the magnetic field

Analysis procedure

In the absence of motion, the ^{2}H NMR signals of a deuteron are separated by a quadrupolar splitting $\Delta\nu_q$ that can be related to the orientation of the carbon-deuterium bond relative to the applied magnetic field using the equation:

$$\Delta\nu_q = \left(\frac{3}{2}\right)\left(\frac{e^2qQ}{h}\right)\left(\frac{1}{2}\left[3\cos^2\theta - 1\right]\right)$$

The magnitude, but not the sign, of $\Delta\nu_q$ can be determined experimentally. The ratio e^2qQ/h is the quadrupolar coupling constant (QCC), and θ is the angle between the magnetic field and the C-D bond direction (see also Table 1). Aliphatic carbon-deuterium bonds have a QCC of 168 kHz (Burnett and Muller, 1971) in a static situation in which there is no motional averaging. In the case of oriented gramicidin A in lipids, an 8% reduction of this value is sufficient to account for wobbling motions of the backbone (Hing et al., 1990; Prosser et al., 1991; Killian et al., 1992). Because the WALP19 α-helix is likely to exhibit at least as much backbone motion as the gramicidin β-helix, most of our calculations employ a reduced value of 155 kHz (92% of 168 kHz); nevertheless, calculations that used either the static value of 168 kHz, or a further reduced value of 140, led to similar conclusions. The very rapid rotation of the alanine methyl group results in a local motional averaging of the methyl deuteron splitting, equivalent to multiplying the quadrupolar coupling constant by $-\frac{1}{3}$ (Killian et al., 1992). (Deviation of the methyl group from an ideal tetrahedral geometry might slightly modify this effective QCC.) Also in this case, θ is defined as the angle between the magnetic field and the C_α-C_β bond of the alanine. Additional motional averaging is caused by rapid axial reorientation around the membrane normal, as is typical of components in liquid crystalline bilayers. When the axis of motional averaging (i.e., the membrane normal) is aligned with the magnetic field, the observed splittings are not affected by this motion. However, when $\beta = 90°$ (defined above) this motion reduces the splittings of all affected signals by 50%, relative to their quadrupolar splitting at $\beta = 0°$.

In the context of an α-helical peptide, several characteristics influence the observed quadrupolar splittings. For the rapidly rotating CD_3 group, for instance, the θ angle is dictated by the precise local direction of the C_α-C_β bond as well as by the global helix orientation. The local side-chain orientation can be characterized by defining two separate angles, one along the helix direction ($\epsilon_\parallel$) and another within the plane perpendicular to the helix direction ($\epsilon_\perp$). For our initial structural model, we used the amino acid library associated with the molecular modeling program Insight II v2000 (Accelrys, Princeton NJ), which assigned to alanines in an α-helix the values $\epsilon_\parallel = 56.2°$ and $\epsilon_\perp = 43.3°$ (Fig. 1, *A* and *B*). Similarly, Jones et al. (1998) reported using Insight II to obtain values of 56° for $\epsilon_\parallel$ and 37.4° for $\epsilon_\perp$. Interestingly, for the β-carbons of 17 other amino acids (excluding glycine and proline) in α-helices, the Insight II library assigns values that range from 55° to 60° for $\epsilon_\parallel$ and from 41° to 48° for $\epsilon_\perp$.

Using the WALP19 model for determining the relative orientations of all involved CD_3 bonds, the peptide was allowed to sample a range of possible orientations away from alignment with the membrane normal. The tilted orientation is defined by two parameters: a rotation angle ρ, for rotation around the helical axis, and a tilt angle τ between the helix axis and the membrane normal. We choose ρ as the angle between the direction in which the peptide is tilted and a line that joins the helix center and the C_α-carbon of glycine 1. Fig. 1 *C* illustrates exactly how these angles were used to first rotate and then tilt the helical peptide model. During the calculation, the peptide was rotated to ρ being 0–360°, in steps of 2°, and for each ρ, tilted from τ of 0° to a maximum τ of 45°, in steps of 0.2°. Additional calculations were performed in which also the uniform local geometry of all alanine side chains was changed, by varying the position of C_β while keeping both the bond length and the C_α position fixed. These calculations varied $\epsilon_\parallel$ by up to 5° from the initial side-chain orientation; allowing a larger change was physically unreasonable and did not yield any additional solutions. The perpendicular angle $\epsilon_\perp$ was kept at the initial value, because a change in this parameter is geometrically indistinguishable from changing ρ. The potential variation in $\epsilon_\perp$ is not expected to significantly affect the final conclusion of our analysis, however (see Discussion).

For each fixed conformation, defined by (τ, ρ) and $\epsilon_\parallel$, one can determine the angle of each of the C_α-$C_\beta D_3$ bonds with respect to the magnetic field and calculate the corresponding quadrupolar splittings. Each conformation is characterized by an error represented by the square root of the mean squared difference (RMSD) between the calculated values and the actually measured splittings. These error values were used to compare the quality of fit for each combination of local helix geometry and global helix orientation.

RESULTS

Sample alignment

The lipids in each sample were well aligned, as determined by solid-state ^{31}P NMR. As an example, the ^{31}P NMR spectra for samples of DOPC with and without 5 mol % WALP19 are shown in Fig. 2. The spectra for $\beta = 0°$ show an intense low field peak due to the lipids in the oriented bilayers in both samples. A small additional NMR signal with a high field maximum can be seen, indicating the presence of a minor population of non-oriented lipids. The aligned lipid fraction constitutes ~90% of the signal intensity, regardless of whether or not 5 mol % WALP19 is present in the liquid-crystalline lipid sample. The spectra at $\beta = 90°$ reconfirm the alignment. The lipid alignment of samples containing DLPC or DMPC was generally similar to, or better than, that of the DOPC samples (results not shown).

WALP19-A^7-d$_4$ in DOPC

The orientation of the membrane-spanning WALP19 peptide was studied by ^{2}H NMR when $\beta = 90°$ or $\beta = 0°$. One expects two pairs of peaks for an Ala-d_4-labeled peptide: an intense doublet for the rapidly rotating C_β methyl group and a weaker doublet for the backbone deuteron, attached to the C_α carbon. For a completely rigid, standard α-helix that is perfectly aligned with the membrane normal, the θ angles would be identical to the angles that the alanine C_α-D and C_α-C_β bonds make with the helix axis. Based on the initial model α-helical structure, from the Insight II library, $\epsilon_\parallel$ was

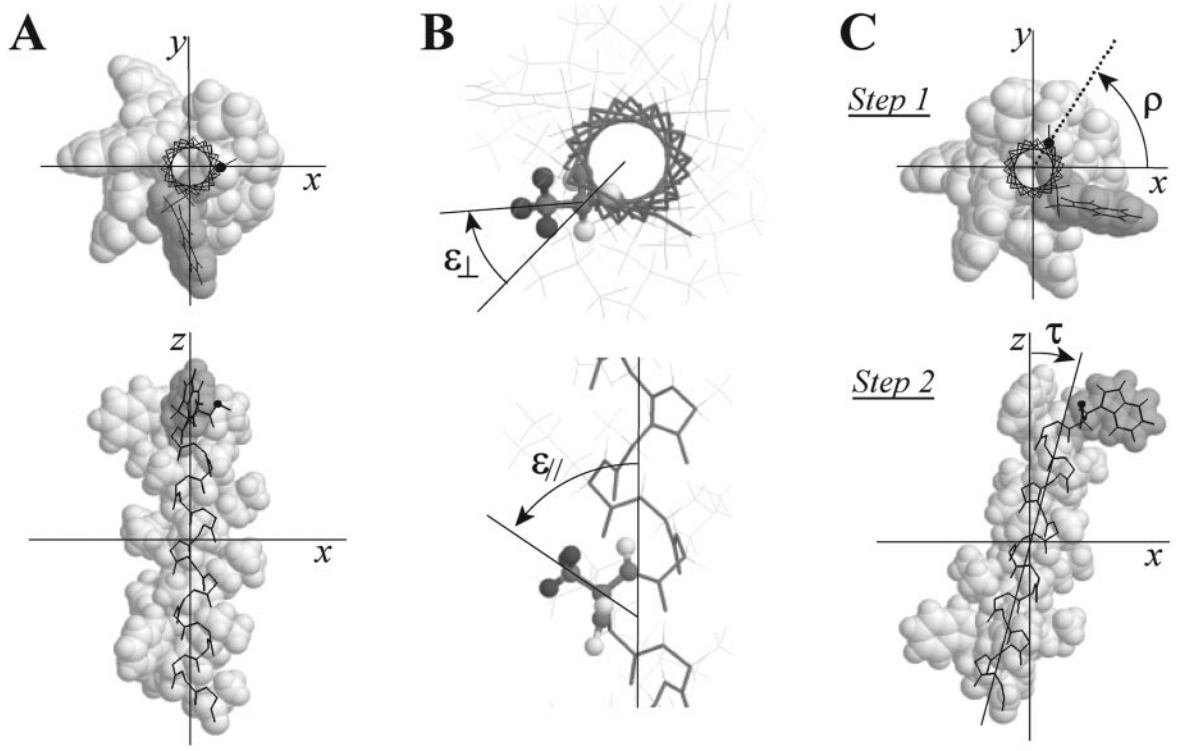

FIGURE 1 Parameters to define helix geometry and orientation. (*A*) Schematic representation of the WALP19 α-helix, illustrating the initial conformation used in the calculations. The *z* axis is defined parallel to the membrane normal, and the peptide helix axis is aligned with this direction. The *x* axis is set to intersect with the C_α of glycine 1 (indicated by a black dot). (*B*) Definition of angles $\epsilon_\parallel$ and $\epsilon_\perp$ that describe the Ala side-chain orientation. $\epsilon_\parallel$ is the angle between the C_α-C_β vector and the helix axis, whereas $\epsilon_\perp$ is the angle with the vector pointing from the helix center through the C_α atom. (*C*) Rotation and subsequent tilting of the helix. The top figure shows a rotation of the helix by ρ degrees. A subsequent tilt by τ degrees yields the final orientation, as shown in the bottom figure. The *z* axis remains aligned with the membrane normal. One tryptophan and the backbone atoms are shown in a black stick representation, with the Gly_1 C_α shown as a black dot.

61.4° for the alanine C_α-D bond, and $\epsilon_\parallel$ was 56.2° for the C_α-C_β bond. These angles would correspond to 39-kHz and 3-kHz quadrupolar splittings, respectively, for the $\beta = 0°$ sample orientation, using an effective QCC of -52 kHz. Fig. 2 shows ^{2}H NMR spectra for WALP19-A^7-d_4 in DOPC. The $\beta = 0°$ spectrum contains a high-intensity doublet with a quadrupolar splitting $|\Delta\nu_q|$ of 11.4 kHz. When $\beta = 90°$, a high intensity doublet is observed with $|\Delta\nu_q|$ of 5.8 kHz. These intense signals are assigned to the deuterons of the alanine side-chain methyl group. Thus, the quadrupolar splitting deviates significantly from the value expected for a nontilted standard α-helix. The observed factor-of-two reduction in $|\Delta\nu_q|$ is consistent with a rapid uniaxial reorientation of the peptide around the membrane normal, as expected for oriented peptides in liquid-crystalline bilayers. The relatively narrow lineshape of these peaks suggests that the peptide adopts one clearly defined orientation within the bilayer, although the possible occurrence of multiple orientations that undergo fast motional averaging (relative to the NMR timescale) cannot be excluded.

Unfortunately, the backbone signals could not be observed for this sample. In addition to their weak intensities, it is possible that the backbone deuterons have a much

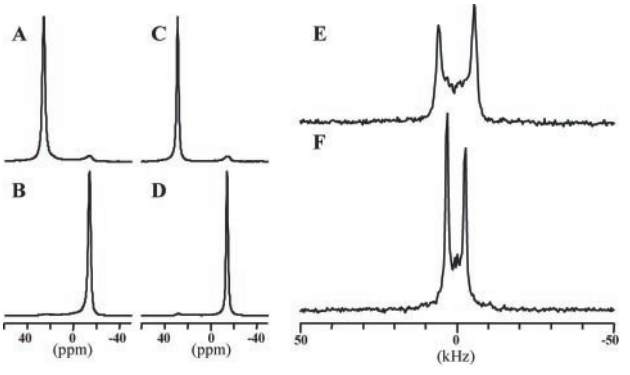

FIGURE 2 NMR measurements of samples consisting of WALP19 in oriented liquid-crystalline DOPC bilayers, at $\beta = 0°$ (*A*, *C*, and *E*) and $\beta = 90°$ sample orientations (*B*, *D*, and *F*). The ^{31}P NMR spectra of the oriented bilayers, either with 5 mol % WALP19 incorporated (*A* and *B*) or without peptide (*C* and *D*), indicate that the lipids are highly aligned on the glass plates, both in the presence and absence of peptide. The ^{2}H NMR spectra of 5 mol % WALP19-A^7-d_4 in DOPC bilayers (*E* and *F* on the same absolute intensity scale) contain a well defined doublet, ascribed to the labeled methyl group. The twofold reduction in quadrupolar splitting of this doublet at $\beta = 90°$ (*F*), compared with $\beta = 0°$, shows that the peptides undergo rapid uniaxial reorientation around the normal to the oriented membrane. All measurements were performed at 40°C.

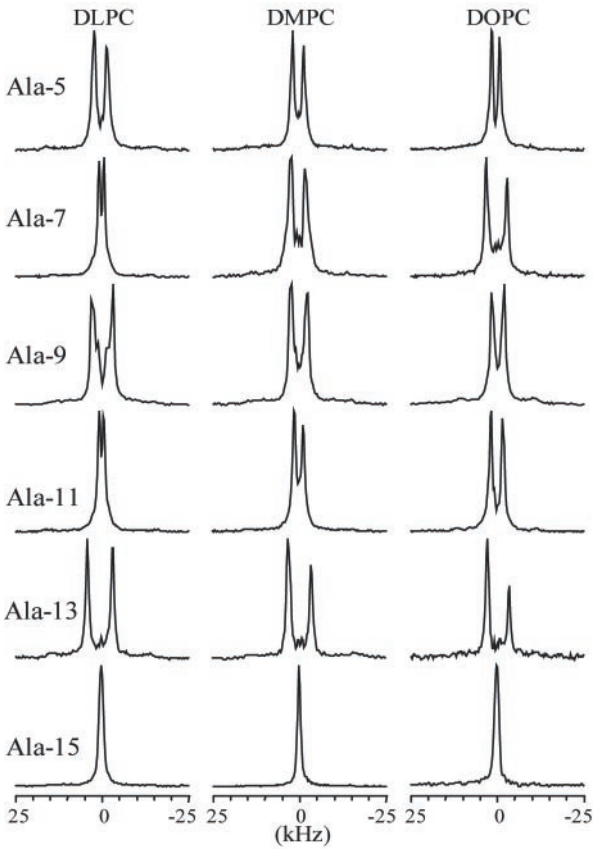

FIGURE 3 ^{2}H NMR spectra of WALP19-A^x-d$_4$ aligned in the three lipids DLPC, DMPC, and DOPC. The sample orientation in all of these experiments is $\beta = 90°$, and all lipids are in the liquid-crystalline phase at the experimental temperature of 40°C.

larger longitudinal relaxation time than the methyl groups, but even when using longer interpulse times, we were unable to observe backbone signals. The situation stands in contrast to oriented transmembrane gramicidin channels, for which C_α-^{2}H backbone deuterons consistently are observed at quadrupolar splittings that uniformly indicate a β-helix in near perfect alignment with the bilayer normal (zero tilt) (Killian et al., 1992; Lee et al., 1995; Jude et al., 1999). Due to the lack of C_α-^{2}H signals, only the methyl group peaks can be used for geometric analysis. The quadrupolar splitting of the methyl doublet of alanine 7 is significantly larger than the expected value for an untilted α-helix. Such a deviation could be indicative of a number of different scenarios. Labeling several different alanines within the WALP19 sequence allows a more detailed analysis.

Multiple alanine labels

WALP19 peptides containing a ^{2}H-labeled alanine at position 5, 7, 9, 11, 13, or 15 were incorporated within oriented lipid bilayers and examined by ^{2}H NMR. Fig. 3 shows the $\beta = 90°$ spectra for each differently labeled peptide in DLPC, DMPC, and DOPC. In some cases low-intensity signals were observed at both sample orientations and were ascribed to the methyl groups in a minor fraction of nonaligned peptide. As for WALP19-A^7-d$_4$ in DOPC, unambiguously assignable backbone peaks were not observed in these spectra. At $\beta = 0°$, the (methyl) signals had quadrupolar splittings twice as large as observed in the displayed spectra at $\beta = 90°$. Those splittings at $\beta = 0°$ are listed in Table 2. Based on repeated measurements and duplicate preparations of several of the samples, the experimental error in $|\Delta\nu_q|$ is estimated to be ± 0.5 kHz. This equates to $\sim \pm 0.26°$ difference in θ angle. The observed differences as functions of alanine sequence position and lipid environment are much larger than this experimental error.

TABLE 2 Magnitudes of methyl group quadrupolar splittings observed for deuterated alanines at positions 5, 7, 9, 11, 13, and 15 in WALP19

Peptide WALP19-A^x-d4	$\|\Delta\nu_q\|$ (kHz)		
	DLPC	DMPC	DOPC
Ala-5	7.2	6.6	4.4
Ala-7	3.3	7.8	11.4
Ala-9	11.3	8.7	7.0
Ala-11	2.6	4.6	6.8
Ala-13	14.0	12.8	11.9
Ala-15	0.0	0.0	1.5

All $|\Delta\nu_q|$ values are for a $\beta = 0°$ sample orientation and a temperature of 40°C. The experimental errors in these values are $\sim$0.5 kHz.

Based on the initial model structure of a nontilted α-helix, each alanine methyl group should give an identical splitting of $\sim$3 kHz, independent of sequence position. Alternatively, a tilted, but straight helix that rotates rapidly around its own axis also would give identical $|\Delta\nu_q|$ values for all of its alanines, with the value determined by the helix orientation. A significant variation in the quadrupolar splittings was observed however, showing a specific trend that correlates well with the positions of the alanines on a helical wheel plot (see Fig. 4). This trend is the basis for the more detailed quantitative investigation that follows.

Analysis: spectral fitting

The model of a straight but tilted helix was used in an initial simulation of the observed data. Limited global motional averaging was simulated by using a reduced effective QCC of $-155/3$ kHz. The initial calculations, based on an unmodified WALP19 model from the Insight II library, yielded a similar optimal peptide orientation in each lipid. These best fits have low τ tilt angles, 4.0° in DLPC, 4.4° in DMPC, and 4.6° in DOPC, and a rotational angle ρ of between 122° and 130°. For each lipid, Fig. 4 *A* graphs the helical-wheel-position dependence of the methyl groups' quadrupolar splittings, both for the theoretical peptide models and the experimental data. Despite a general match

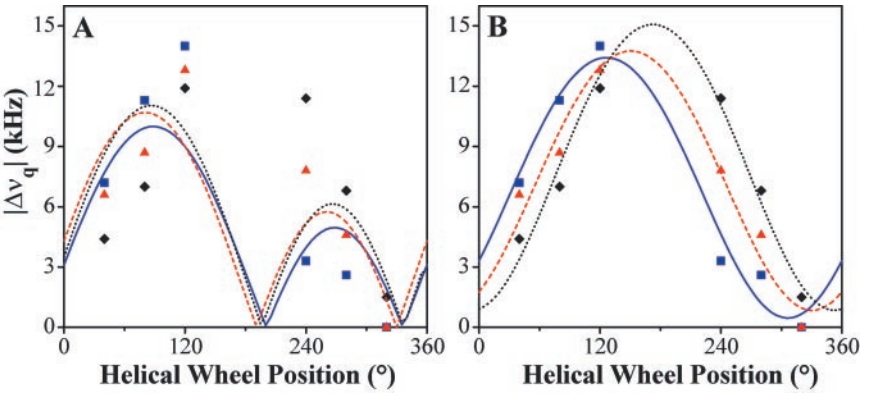

FIGURE 4 Comparison of experimental and theoretical ^{2}H NMR quadrupolar splittings $|\Delta\nu_q|$. (*A*) Optimal solutions found using the initial Ala side-chain angle of $\epsilon_{\|} = 56.2°$ from the Insight II library. (*B*) The same as *A* after fine tuning of this parameter. The lines represent the theoretical graphs on which the quadrupolar splittings of the alanines would lie, for the predicted WALP19 orientation in DLPC (*solid blue line*), DMPC (*dashed red line*), and DOPC (*dotted black line*). The measured data are shown as squares, triangles, and diamonds, respectively.

between experiment and simulation, the associated RMSD errors, between 2.4 and 3.7 kHz, are much larger than expected based on the experimental errors.

Additional fine-tuning of the simulation was performed by allowing small deviations of the alanine CD_3 groups from their orientation in the initial library model, by up to 5° in $\epsilon_{\|}$. This minor adjustment led to a significant improvement of the fits to the data, indicated by large reductions of the RMSD values. The best results were observed for $\epsilon_{\|}$ angles (identical for each alanine in the helix) of 58.6° in DLPC, 58.8° in DMPC, and 59.2° in DOPC (see Table 3). Whether this apparent trend from lipid to lipid has physical significance is unclear. The RMSD values are reduced to less than 1 kHz, in agreement with the errors in the experimental measurements. Such deviations correspond to a deviation in the θ angles of less than 0.5°. The obtained peptide orientations have a slightly reduced tilt angle τ of between 3.6° and 4.0° and rotational angles ρ that are offset by 40–90° from the preliminary values. Fig. 4 *B* displays the comparison of these improved fits with the experimental results, illustrating the high level of matching that was obtained with these structural parameters.

These final simulations were examined in more detail by graphing the RMSD errors for all tilt and rotation angles, using contour plots (Fig. 5). The calculations were performed with $\epsilon_{\|}$ of the methyl groups set to each of the optimal angles as listed in Table 3. As before, the $\epsilon_{\perp}$ angle was kept at its original value. The contour plots clearly indicate a preference for one well defined orientation in all lipids. It is furthermore clear that the error is significantly more sensitive to changes in τ than to changes in ρ.

Analysis: dynamics/motion

The calculations described above were performed using an effective QCC of $-(0.92 \times 168\ \text{kHz})/3 = -52$ kHz, to simulate a similar extent of overall motional averaging, as has been reported for the backbone of gramicidin channels. To explore the effect of an uncertainty in the exact value of the QCC, the calculations were also performed with QCCs of −56 and −47 kHz. A value of −56 kHz is equivalent with a static situation, and the −47-kHz value signifies a significantly larger motion than seen in gramicidin. As seen in Table 3, using these two extremes leads to only minor changes in the τ and $\epsilon_{\|}$ angles, whereas the rotational angles and RMSD values remain largely unaffected. These data show that even if the actual dynamics of the peptide deviate from our primary assumption, the results remain valid.

DISCUSSION

The tryptophans of WALP peptides exhibit affinity for the membrane-water interface and are responsible for anchoring the peptides in approximately transmembrane orientations. WALP peptides were the first membrane-spanning α-helical peptides that were shown to influence phospholipid phase behavior as a function of the relative hydrophobic

TABLE 3 WALP19 orientations in DLPC, DMPC, and DOPC

	DLPC			DMPC			DOPC		
QCC (kHz)	(τ, ρ)	$\varepsilon_{\|}$	RMSD (kHz)	(τ, ρ)	$\varepsilon_{\|}$	RMSD (kHz)	(τ, ρ)	$\varepsilon_{\|}$	RMSD (kHz)
−47	(4.0, 172)	59.0	0.87	(4.0, 196)	59.2	0.84	(4.4, 212)	59.6	0.66
−52	(3.6, 172)	58.6	0.87	(3.6, 194)	58.8	0.83	(4.0, 216)	59.2	0.66
−56	(3.4, 172)	58.2	0.86	(3.4, 192)	58.6	0.85	(3.6, 210)	58.8	0.66

The combination of tilt (τ) and rotation (ρ) angles defines the optimal helix orientation, and the angle $\varepsilon_{\|}$ describes the optimal alanine side-chain conformation (for all labeled alanines in the helix). The error value indicates the difference between the calculated and measured splittings, expressed as the RMSD.

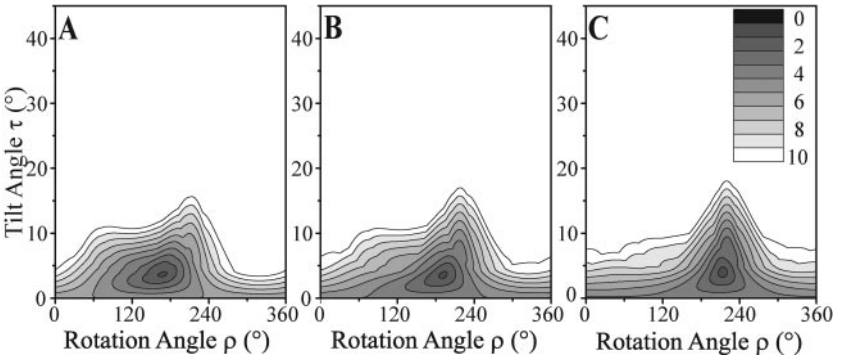

FIGURE 5 Conformational dependence of the quality of fit. (*A*—*C*) The error in the three lipids DLPC, DMPC, and DOPC varies as a function of the peptide tilt and rotation. The contour levels indicate conformations with a RMSD between the calculated and measured splittings of 0–10 kHz. These results were obtained using the optimized alanine side-chain geometries and a QCC of −52 kHz.

lengths of the peptide and lipid molecules (Killian et al., 1996). In this article, we have examined the WALP19 orientation with respect to the membrane normal in more precise detail than was previously possible using CD or polarized ATR-FTIR.

Measurements using two different sample orientations ($\beta = 0°$ and 90°) indicate that the peptides experience rapid axial reorientation about the membrane normal, typical of fluid membrane components. The magnitude of the quadrupolar splittings and their variation with sequence position indicate that the peptide is restricted from experiencing rapid reorientation around its own axis and has a small nonzero tilt away from the membrane normal. Remarkably, this tilt was found to be close to 4°, seemingly independent of the lipid environment in which the peptide is imbedded. The main difference between the lipid systems is the way the peptide is rotated within the membrane. Fig. 6 shows the WALP19 orientations in DLPC and DOPC to illustrate the (small) peptide adjustments in the different lipid systems and for comparison with the untilted conformation.

A central issue in the GALA calculations is the position dependence of the CD_3 quadrupolar splittings. Fig. 7 illustrates how each parameter influences different aspects of the sequence dependence. The cylindrical nature of the helix dictates that the splittings should follow a sine-shaped curve. The amplitude of this curve is determined by the peptide tilt τ, the phase is determined mostly by the peptide rotational angle ρ, and the zero level of the sine wave is equal to the expected quadrupolar splitting for the untilted peptide. This latter parameter is determined by the helical structure itself, specifically by the $\epsilon_{\|}$ angle that defines the precise orientation of the alanine side chain relative to the helix axis. Because each different parameter affects a different aspect of the theoretical curve, it was possible to

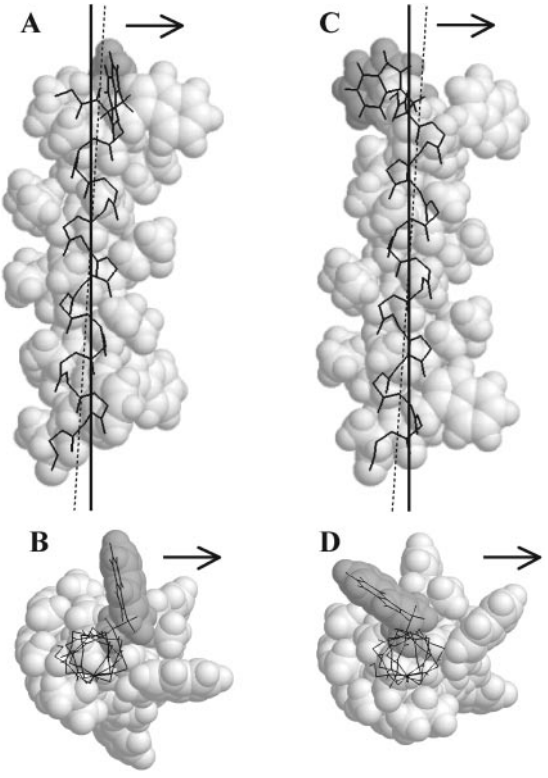

FIGURE 6 Schematic representation of the WALP19 orientations in DLPC (*A* and *B*) and DOPC (*C* and *D*). (*A* and *C*) A side view from a direction perpendicular to the plane in which the peptide is tilted, with the membrane normal indicated by a solid line and the helix axis by a dashed line. (*B* and *D*) Corresponding top views as seen down the membrane normal. The backbone and one tryptophan are shown in a black stick representation. The arrows indicate the direction of tilt.

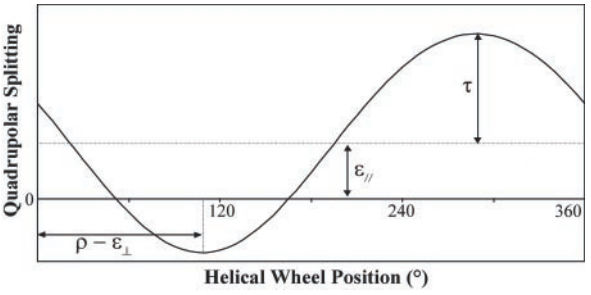

FIGURE 7 Dependence of the $\Delta\nu_q$ trend on helical wheel position and structural parameters. This figure illustrates how the different conformational and structural parameters used in this study affect the dependence of the splitting on helical wheel position. The predominant factors affecting each characteristic of the sine curve are noted in the figure (see text for additional details).

optimize each of them independently based on our experimental data. One complication is that the sine phase is also dependent on the $\epsilon_\perp$ angle. However, we observed a relatively large uncertainty in the ρ angle and expect any deviation of the $\epsilon_\perp$ angle to be small, as is the case for the $\epsilon_\parallel$ angle. This suggests that not knowing the exact value of $\epsilon_\perp$ does not affect the general conclusions. Other experiments will be necessary to study this parameter.

We found that the best fit was obtained when the $\epsilon_\parallel$ side-chain angles were set to ~58.8°. At ~2.6° from the original alanine angle in the Insight II library, this is well within the range of angles assigned for the different types of amino acids. This partial geometrical analysis of the α-helical conformation of this peptide is remarkable both because of its apparent large sensitivity and the fact that it was done with the peptide present in the hydrophobic core of the lipid bilayer. It is conceivable that this environment could affect the precise helical conformation and cause it to differ slightly from a similar helix in a more hydrophilic environment. Such detailed information could be important for increasingly detailed examination of membrane protein structures and their interactions with each other and other membrane components. (We note that $\epsilon_\parallel$ will be sensitive to small adjustments in the backbone ϕ and ψ angles. Although standard protein structure refinement strategies do not refine this parameter directly, a precise value for $\epsilon_\parallel$ could nevertheless be included as an additional constraint during the refinement of some α-helical portions of structures.)

The membrane is known to be a highly dynamic environment. Our ^{2}H NMR results are nevertheless consistent with a tilted peptide that is motionally restricted. A restricted (or slow) motion of a membrane-spanning peptide was similarly observed in the examination of the epidermal growth factor receptor (Jones et al., 1998). The simulated reductions in QCC could correspond to limited transient and local fluctuations in the α-helical structure, limited whole-molecule motions, or even deviations of the methyl groups from perfect tetrahedral geometry. Other possible types of global motion would involve dynamic variations in the tilt and/or rotation angles. Our data are inconsistent with a rapid full rotation around the helix director, but the contour plots in Fig. 5 do show that the error level is more tolerant of changes in ρ than in τ. This finding would suggest that whereas the tilt angle is relatively well defined, a larger uncertainty, or slippage, is permissible for the rotational angle. Some specific motions that were simulated, such as a jumping motion (alternating between two specific ρ angles) or a rolling motion (sampling a range of ρ-values), did not significantly improve the calculated fits (results not shown).

In a format inspired by the PISEMA/PISA wheel diagrams that so elegantly illustrate the determined tilt direction (Marassi and Opella, 2000; Wang et al., 2000), a graphical representation of our data is shown in Fig. 8. A polar graph was used to produce a circular plot of the dependence of the quadrupolar splitting on the position in a helical wheel (the magnitude of $|\Delta\nu_q|$ is indicated by the distance from the graph origin). The experimental data and the calculated curves are shown as colored data points and lines, respectively. The figure illustrates that alanines characterized by a large splitting are localized on one side of the helix, close to the direction of peptide tilt (indicated by the colored arrows). More precisely, the exact direction of tilt is 43° (i.e., $\epsilon_\perp$) farther along the helical wheel than the maximum on the theoretical $\Delta\nu_q$ curve, as illustrated in the figure for DOPC (black lines). This reflects the fact that the peptide tilt causes the alanines on that side of the helix to have their methyl groups oriented the farthest away from the magic angle. Fig. 8 also allows one to examine the distribution of the different amino acids around the helix and relative to the direction of tilt. In WALP19 the tryptophan interfacial anchors are all found on one side of the helical wheel. Remarkably, in each of the lipids, the peptide tilt appears to be directed toward this side of the helix.

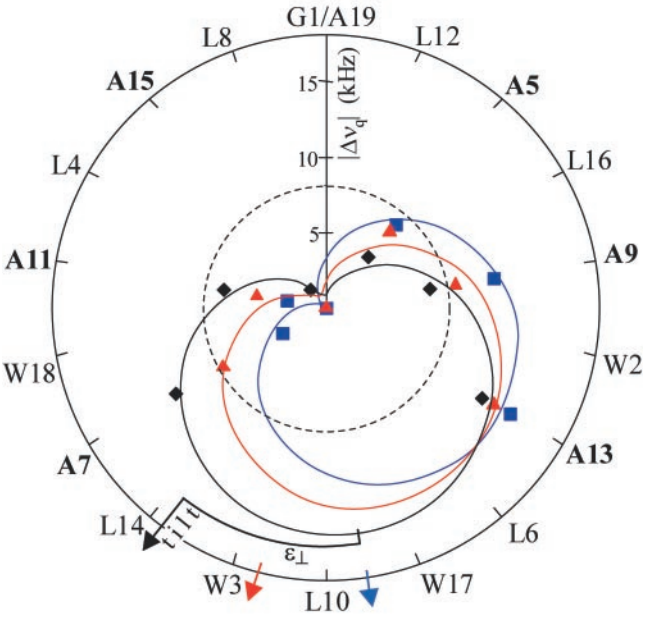

FIGURE 8 Polar coordinates were used to chart the magnitude of $|\Delta\nu_q|$ as it varies around the helical wheel. Quadrupolar splittings of 0 kHz are located on the origin. The magnitude of other splittings is indicated by the distance from the graph's origin, in the direction of the alanine positions indicated along the outside perimeter. Data points are shown as squares (DLPC), triangles (DMPC), and diamonds (DOPC). The curves indicate the best-fit values. The position-independent $\Delta\nu_q$ for the untilted peptide is shown as a dashed circle (for $\epsilon_\parallel \approx 59°$). Colored arrows indicate the direction of tilt in the different lipids (see text for additional details).

An intriguing question relates to what factors could cause the peptide to adopt such a specifically preferred and motionally restricted orientation. Although complex membrane proteins largely determine their structures through interactions of adjacent transmembrane helices, our system has been shown to experience relatively little aggregation (de

Planque et al., 1998). If WALP19 does dimerize, the narrowness of the observed peaks would suggest that both peptides are equivalent and in an identical orientation to the magnetic field. Such a dimer would rotate freely around its symmetry axis (which could be the membrane normal), whereas the peptides would be fixed relative to each other, with an approximate 8° crossing angle. However, such an angle would seem quite small for traditional knobs-in-holes side-chain packing, and it is not clear what other interactions would be available to stabilize such a dimer.

The orientation could also be determined by peptide-lipid interactions. A positive hydrophobic mismatch of a transmembrane peptide with a thinner lipid bilayer is one potential cause for tilting (Killian, 1998; Harzer and Bechinger, 2000). The hydrophobic thicknesses, defined as the distance between the C-2 carbons of the acyl chains, of DLPC, DMPC, and DOPC are ~24 Å, ~26 Å, and ~27 Å, respectively (Nagle and Tristram-Nagle, 2000). Unexpectedly, we see very minor changes in tilt orientation under this range of conditions, and we even observe a peptide tilt in the thickest bilayer. Also, even a 5° tilt of WALP19 would only change its effective transmembrane hydrophobic length by roughly 0.1 Å (the difference in projection along the membrane normal for a peptide of 19 residues, i.e., 19×1.5 Å). This will hardly be able to compensate for a hydrophobic mismatch estimated to be several angstroms. Our experiments therefore seem to agree with previous experiments that already have indicated that mismatch conditions cause the lipids to adjust, rather than the peptides. WALP19 causes the order parameter of the lipid acyl chains of DLPC and DMPC to increase, suggesting changes in lipid dynamics or the effective acyl chain length in response to the presence of WALP19 (de Planque et al., 1998).

Because the peptide tilt is relatively insensitive to the bilayer thickness, it appears that the peptide orientation might be largely determined by features common to all three lipids or by characteristics inherent to the peptide itself. For instance, the surface pattern caused by the alternating alanine and leucine residues might optimally interact with the lipid acyl chains in a specific tilted orientation of the peptide. Such a relation between surface characteristics and transmembrane peptide behavior has recently been suggested (Lewis et al., 2001; Zhang et al., 2001). Another important characteristic is the presence of tandem tryptophan residues asymmetrically situated at the extremities. (Although two tryptophans are present near each end of WALP19, their dispositions with respect to the directional backbone will be different at the N- and C-terminals.) These membrane interface anchors are thought to have a specific preferred orientation in their interaction with the membrane interfacial region (Yau et al., 1998), which should be similar in all three lipids (Persson et al., 1998). To achieve quasi-equivalent orientations for each indole ring, the peptide could change its tilt and/or exploit the inherent flexibility of the tryptophan side chains (Petrache et al., 2002). The role of the tilt would be to change the direction and depth of the (backbone-linked) C_α-C_β bonds relative to the membrane. Naturally, with the small tilt angles found in this study, the effect on these bond orientations is relatively subtle, in the range of at most several degrees. Nevertheless, small adjustments in τ and ρ might still allow the actual indole rings access to more favorable environments and orientations. The need to maintain a specific, optimized orientation for each of these bulky aromatic side chains could also explain the resistance of the peptide to reorientation around its own axis. Examination of the behavior of labeled tryptophan side chains in these peptides would enable further evaluation of these ideas.

CONCLUSION

It was shown here that the geometric analysis of labeled alanines (GALA) by solid-state ^{2}H NMR can be used to place narrow limits on the orientation, conformation, and lipid interactions of membrane-spanning peptides. Although the flanking tryptophans indeed do anchor WALP19 in an approximately transmembrane orientation, ^{2}H NMR spectra from labeled alanines nevertheless are consistent with a distinctly nonzero yet small tilt angle of ~4° for WALP19 in three different phosphatidylcholines. The tilt seems relatively insensitive to the bilayer thickness or hydrophobic mismatch, suggesting that the peptide orientation is largely determined by characteristics inherent to the peptide itself. A complete rationale for this behavior remains elusive but could include an important role for the anchoring tryptophans. We were furthermore able to obtain some detailed structural data on the helical geometry of a bilayer-traversing peptide. These observations may provide insight concerning the early stages of membrane protein assembly for they illustrate that, even in the absence of extensive protein-protein interactions, segments of a membrane protein should be predisposed toward specific conformations and orientations.

We thank Denise V. Greathouse and Matthew J. Whitley for valuable contributions to the experiments and preparation of the manuscript.

This work was supported in part by National Institutes of Health grant GM34968.

REFERENCES

Bowie, J. U. 1997. Helix packing in membrane proteins. *J. Mol. Biol.* 272:780–789.

Burnett, L. J., and B. H. Muller. 1971. Deuteron quadrupole coupling constants in three solid deuterated paraffin hydrocarbons: C_2D_6, C_4D_{10}, and C_6D_{14}. *J. Chem. Phys.* 55:5829–5831.

Cornell, B. A., F. Separovic, A. J. Baldassi, and R. Smith. 1988. Conformation and orientation of gramicidin A in oriented phospholipid bilayers measured by solid state carbon-13 NMR. *Biophys. J.* 53:67–76.

Davis, J. H., K. R. Jeffrey, M. I. Valic, Bloom, and T. P. Higgs. 1976. Quadrupolar echo deuteron magnetic resonance spectroscopy in ordered hydrocarbon chains. *Chem. Phys. Lett.* 42:390–394.

de Planque, M. R. R., E. Goormaghtigh, D. V. Greathouse, R. E. Koeppe II, J. A. W. Kruijtzer, R. M. J. Liskamp, B. de Kruijff, and J. A. Killian. 2001. Sensitivity of single membrane-spanning α-helical peptides to hydrophobic mismatch with a lipid bilayer: effects on backbone structure, orientation, and extent of membrane incorporation. *Biochemistry.* 40:5000–5010.

de Planque, M. R. R., D. V. Greathouse, R. E. Koeppe II, H. Schäfer, D. Marsh, and J. A. Killian. 1998. Influence of lipid/peptide hydrophobic mismatch on the thickness of diacylphosphatidylcholine bilayers. a ^{2}H NMR and ESR study using designed transmembrane alpha-helical peptides and gramicidin A. *Biochemistry.* 37:9333–9345.

de Planque, M. R. R., J. A. W. Kruijtzer, R. M. J. Liskamp, D. Marsh, D. V. Greathouse, R. E. Koeppe II, B. de Kruijff, and J. A. Killian. 1999. Different membrane anchoring positions of tryptophan and lysine in synthetic transmembrane α-helical peptides. *J. Biol. Chem.* 274: 20839–20846.

Demmers, J. A. A., J. Haverkamp, A. J. R. Heck, R. E. Koeppe II, and J. A. Killian. 2000. Electrospray ionization mass spectrometry as a tool to analyze hydrogen/deuterium exchange kinetics of transmembrane peptides in lipid bilayers. *Proc. Natl. Acad. Sci. U.S.A.* 97:3189–3194.

Demmers, J. A. A., E. van Duijn, J. Haverkamp, D. V. Greathouse, R. E. Koeppe II, A. J. R. Heck, and J. A. Killian. 2001. Interfacial positioning and stability of transmembrane peptides in lipid bilayers studied by combining hydrogen/deuterium exchange and mass spectrometry. *J. Biol. Chem.* 276:34501–34508.

Greathouse, D. V., R. L. Goforth, T. Crawford, P. C. A. van der Wel, and J. A. Killian. 2001. Optimized aminolysis conditions for cleavage of N-protected hydrophobic peptides from solid-phase resins. *J. Pept. Res.* 57:519–527.

Greathouse, D. V., R. E. Koeppe II, L. L. Providence, S. Shobana, and O. S. Andersen. 1999. Design and characterization of gramicidin channels. *Methods Enzymol.* 294:525–550.

Haltia, T., and E. Freire. 1995. Forces and factors that contribute to the structural stability of membrane proteins. *Biochim. Biophys. Acta.* 1228: 1–27.

Harzer, U., and B. Bechinger. 2000. Alignment of lysine-anchored membrane peptides under conditions of hydrophobic mismatch: a CD, ^{15}N and ^{31}P solid-state NMR spectroscopy investigation. *Biochemistry.* 39: 13106–13114.

Hing, A. W., S. P. Adams, D. F. Silbert, and R. E. Norberg. 1990. Deuterium NMR of Val^1···(2- ^{2}H)Ala^3···gramicidin A in oriented DMPC bilayers. *Biochemistry.* 29:4144–4156.

Jones, D. H., K. R. Barber, E. W. VanDerLoo, and C. W. M. Grant. 1998. Epidermal growth factor receptor transmembrane domain: ^{2}H NMR implications for orientation and motion in a bilayer environment. *Biochemistry.* 37:16780–16787.

Jude, A. R., D. V. Greathouse, M. C. Leister, and R. E. Koeppe, II. 1999. Steric interactions of valines 1, 5, and 7 in [valine 5, D-alanine 8] gramicidin A channels. *Biophys. J.* 77:1927–1935.

Killian, J. A. 1998. Hydrophobic mismatch between proteins and lipids in membranes. *Biochim. Biophys. Acta.* 1376:401–415.

Killian, J. A., I. Salemink, M. de Planque, G. Lindblom, R. E. Koeppe II, and D. V. Greathouse. 1996. Induction of non-bilayer structures in diacylphosphatidylcholine model membranes by transmembrane α-helical peptides: importance of hydrophobic mismatch and proposed role of tryptophans. *Biochemistry.* 35:1037–1045.

Killian, J. A., M. J. Taylor, and R. E. Koeppe, II. 1992. Orientation of the valine-1 side chain of the gramicidin transmembrane channel and implications for channel functioning: a ^{2}H NMR study. *Biochemistry.* 31:11283–11290.

Koeppe, R. E., II, T. C. Vogt, D. V. Greathouse, J. A. Killian, and B. de Kruijff. 1996. Conformation of the acylation site of palmitoylgramicidin in lipid bilayers of dimyristoylphosphatidylcholine. *Biochemistry.* 35: 3641–3648.

Kukol, A., and I. T. Arkin. 1999. *vpu* transmembrane peptide structure obtained by site-specific Fourier transform infrared dichroism and global molecular dynamics searching. *Biophys. J.* 77:1594–1601.

Kukol, A., and I. T. Arkin. 2000. Structure of the *Influenza* C virus CM2 protein transmembrane domain obtained by site-specific infrared dichroism and global molecular dynamics searching. *J. Biol. Chem.* 275: 4225–4229.

Lee, K. C., and T. A. Cross. 1994. Side-chain structure and dynamics at the lipid-protein interface: Val_1 of the gramicidin A channel. *Biophys. J.* 66:1380–1387.

Lee, K. C., S. Huo, and T. A. Cross. 1995. Lipid-peptide interface: valine conformation and dynamics in the gramicidin channel. *Biochemistry.* 34:857–867.

Lewis, R. N. A. H., F. Liu, R. S. Hodges, and R. M. McElhaney. 2001. Interactions of compositionally isomeric $\alpha-$helical transmembrane peptides and phospholipid bilayers. *Biophys. J.* 80:550a.

Marassi, F. M., and S. J. Opella. 2000. A solid-state NMR index of helical membrane protein structure and topology. *J. Magn. Reson.* 144: 150–155.

Nagle, J. F., and S. Tristram-Nagle. 2000. Structure of lipid bilayers. *Biochim. Biophys. Acta.* 1469:159–195.

Persson, S., J. A. Killian, and G. Lindblom. 1998. Molecular ordering of interfacially localized tryptophan analogs in ester- and ether-lipid bilayers studied by ^{2}H-NMR. *Biophys. J.* 75:1365–1371.

Petrache, H. I., D. M. Zuckerman, J. N. Sachs, J. A. Killian, R. E. Koeppe, II, and T. B. Woolf. 2002. Hydrophobic matching mechanism investigated by molecular dynamics simulations. *Langmuir.* 18:1340–1351.

Prosser, R. S., J. H. Davis, F. W. Dahlquist, and M. A. Lindorfer. 1991. ^{2}H nuclear magnetic resonance of the gramicidin A backbone in a phospholipid bilayer. *Biochemistry.* 30:4687–96.

Singer, S. J., and G. L. Nicolson. 1972. The fluid mosaic model of the structure of cell membranes. *Science.* 175:720–731.

Torres, J., A. Kukol, and I. T. Arkin. 2000. Use of a single glycine residue to determinate the tilt and orientation of a transmembrane helix: a new structural label for infrared spectroscopy. *Biophys. J.* 79:3139–3143.

Ulmschneider, M. B., and M. S. P. Sansom. 2001. Amino acid distributions in integral membrane protein structures. *Biochim. Biophys. Acta.* 1512: 1–14.

van der Wel, P. C. A., T. Pott, S. Morein, D. V. Greathouse, R. E. Koeppe, II, and J. A. Killian. 2000. Tryptophan-anchored transmembrane peptides promote formation of nonlamellar phases in phosphatidylethanolamine model membranes in a mismatch-dependent manner. *Biochemistry.* 39:3124–3133.

Wallin, E., and G. von Heijne. 1998. Genome-side analysis of integral membrane proteins from eubacterial, archaean, and eukaryotic organisms. *Protein Sci.* 7:1029–1038.

Wang, J., J. Denny, C. Tian, S. Kim, Y. Mo, F. Kovacs, Z. Song, K. Nishimura, Z. Gan, R. Fu, J. R. Quine, and T. A. Cross. 2000. Imaging membrane protein helical wheels. *J. Magn. Reson.* 144:162–167.

White, S. H., and W. C. Wimley. 1999. Membrane protein folding and stability: physical principles. *Annu. Rev. Biophys. Biomol. Struct.* 28: 319–365.

Yau, W.-M., W. C. Wimley, K. Gawrisch, and S. H. White. 1998. The preference of tryptophan for membrane interfaces. *Biochemistry.* 37: 14713–14718.

Zhang, Y.-P., R. N. A. H. Lewis, R. S. Hodges, and R. N. McElhaney. 2001. Peptide models of the helical hydrophobic transmembrane segments of membrane proteins: interactions of acetyl-K_2-$(LA)_{12}$-K_2-amide with phosphatidylethanolamine bilayer membranes. *Biochemistry.* 40: 474–482.